nature biomedical engineering

SUPPLEMENTARY INFORMATION

https://doi.org/10.1038/s41551-020-0556-3

In the format provided by the authors and unedited.

De novo development of proteolytically resistant therapeutic peptides for oral administration

Xu-Dong Kong[1], Jun Moriya[1], Vanessa Carle[1], Florence Pojer[2], Luciano A. Abriata[2,3], KaycieDeyle[1] and Christian Heinis[1]✉

[1]Institute of Chemical Sciences and Engineering, School of Basic Sciences, Ecole Polytechnique Fédérale de Lausanne (EPFL), Lausanne, Switzerland. [2]Protein Production and Structure Core Facility, School of Life Sciences, Ecole Polytechnique Fédérale de Lausanne (EPFL), Lausanne, Switzerland. [3]Laboratory for Biomolecular Modeling, School of Life Sciences, Ecole Polytechnique Fédérale de Lausanne (EPFL) and Swiss Institute of Bioinformatics, Lausanne, Switzerland. ✉e-mail: christian.heinis@epfl.ch

Table of contents

Supplementary Figures

Supplementary Results

Improving affinity of F3 with unnatural amino acids

A comparison of peptides similar to F3 showed that amino acids in the second peptide ring CCRCP were fully conserved, while the amino acids at the N-terminus and in the first ring were more variable. In a first attempt of activity and stability maturation, we chose to replace the amino acids in the first ring with natural amino acids that emerged at the same positions in the phage-selected peptides, including Asn4→Ser and Met6→Phe (Supplementary Fig. 10). Replacement of Met6 with Phe improved the binding affinity by 4.9-fold, but the stability decreased by 2.8-fold. In a second attempt, we replaced the amino acids in positions Met6, Arg9 and Pro11 with unnatural ones having similar side chains (Fig. 3e and Supplementary Fig. 10). In position Pro11, the replacement with D-Pro improved the affinity 17.3-fold (F18). Finally, we also tested a peptide variant in which we appended to the C-terminus a tryptophan residue because this residue was found to follow proline in several of the phage-selected peptides. The resulting peptide F21 had a 9.5-fold improved K_i (Supplementary Fig. 10). For all variants of F3, the inhibition constant K_i, the activated partial thromboplastin time (aPTT; prolongation compared to no inhibitor control) and the stability in 100% SIF were determined and are shown in Supplementary Fig. 10.

X-ray structures of double-bridged peptides bound to FXIa

The structures of the two peptides F19 and F21 in complex with the catalytic domain of FXIa were determined by X-ray crystallography. As expected based on the similar amino acid sequences, the two peptides F19 and F21 bind to the same site and form the same key interactions with FXIa (Supplementary Fig. 14). The structure of F19, bound to the catalytic domain of FXIa, is discussed in the following.

The double-bridged peptide F19 forms a 3_{10}-helical structure (Fig. 4a). The electron density of the peptide was well defined for all the amino acids as well as the two linkers,

allowing an unambiguous assignment of side chain orientations and the two chemical bridges (Supplementary Fig. 13a). Four intramolecular hydrogen bond interactions are formed between atoms of F19 (Supplementary Fig. 13b). Three of them are formed by the backbone C=O and N-H pairs Asn3-Cys6, Ile4-Cys7 and Cys6-Cys9, indicating a 3_{10}-helix structure. The backbone dihedral angles φ and ψ of residues Ile4-Arg8 shown in the Ramachandran plot in Supplementary Fig. 13c are in line with the 3_{10}-helix structure. Both peptide rings of F19 form contacts with the FXIa catalytic domain, covering a total surface of 649 $Å^2$ (Supplementary Table 2). Fifteen intermolecular hydrogen bonds were identified directly between F19 and FXIa, or through hydrogen bond networks mediated by water molecules in between (Supplementary Fig. 13b). Most of the intermolecular hydrogen bonds are contributed by the residues Arg8 and d-Pro10 from the second ring of F19, showing the importance of these two residues observed in the affinity maturation study.

The FXIa catalytic domain bound to F19 has the same overall structure as the FXIa catalytic domain bound to a small molecule inhibitor (FXIa-benzamidine; PDBID: 1ZHM) wherein several small conformational differences were observed for residues around the substrate-binding site of FXIa (Supplementary Fig. 13d and 13e). Specifically, the backbone of five residues and sidechains of eight residues had significantly moved apart from the catalytic center of FXIa to accommodate F19. Most noteworthy are the sidechain of Ser195, being the nucleophile of the catalytic triad, that rotated by 180° due to the binding of F19, and the sidechain of Arg39 that moved slightly towards the peptide to form a hydrogen bond with d-Pro10.

Structure of peptide F19 in solution

We analyzed F19 by CD and NMR spectroscopy to assess if the peptide adapts a helical conformation when it is not bound to the target. The CD spectra of F19 in water or sodium phosphate buffer (20 mM, pH 7.4) did not show the typical signature for a

3_{10}-helix structure (Fig. 4b). Addition of 40% (v/v) of the helix-promoting solvent trifluoroethanol (TFE) changed the spectrum only slightly. The absence of a helical structure for F19 in aqueous solution was confirmed by NMR analysis. Specifically, no medium range NOEs were observed that would be expected for a helix (Fig. 4c and Supplementary Fig. 15), ^{13}C chemical shifts for Cα and Cβ atoms were very close to random coil values, and the $^{3}J_{HN\text{-}HA}$ couplings of 9 out of 10 residues were higher than 6 Hz (Fig. 4c).

Stability of linear and monocyclic derivatives of F19

In order to understand the structural basis of the high protease resistance of F19, we compared the stability of linear and singly-cyclized peptide derivatives of the double-bridged peptide. The peptides lacking one or both chemical bridges were synthesized without the thiol groups in positions that are not cyclized, to prevent cyclization through disulfide formation. For example the linear form of F19 was synthesized with alanine residues instead of the three cysteine residues and propionic acid (Ala*) instead of mercapto-propionic acid Cys* (F22: A*VNIMAARAp) (Supplementary Fig. 16).

The linear peptide F22 was fully digested within 0.5 min in 10 mg ml^{-1} of pancreatin, while the fragment 'A*VNIM' was further digested with a half-life of 16.9 min. The monocyclic peptide F23, that lacks the second bridge (C*VNIMACRAp; Cys*1 and Cys7 linked by **7**), had a half-life of 1.8 min. An intermediate product being the first ring of the peptide (C*VNIMAC; Cys*1 and Cys7 linked by **7**) had a half-life of > 30 min. The second monocyclic peptide F24, that lacks the second bridge (A*VNIMCARCp; Cys6 and Cys9 linked by **7**) was fully digested to the fragment 'A*VNIM' within 0.5 min. The second ring (CARCp) being a potential degradation product was not detected.

To study the impact of the linker type on the stability, we replaced in F19 the linker **7** with linker **2**. The resulting peptide, F25 showed a slightly decreased inhibition potency

(K_i = 2.6 nM). Interestingly, F25 has a 12.7-fold worse stability ($t_{1/2}$ = 42 min) showing that the chemical bridges and their specific structure have a large impact on the stability.

In addition to the backbone configuration, ring size and linker type, we expected that the amino acid sequence was also critical for the stability. The sequence of the first ring of F19 appeared to be particularly stable as it remained detectable as degradation intermediate as a linear peptide. To assess the importance of the sequence, we inserted in F19 an arginine residue (Asn3 to Arg; C*VRIMCCRCp) which was expected to be easily cleaved by trypsin. The resulting peptide, F26 was rapidly cleaved in the first ring (half-life of < 0.1 min), showing that the amino acid sequence was also important for the stability.

Supplementary Materials and Methods

High-throughput sequencing of phage DNA

Phage plasmid DNA was isolated from 200 μl samples taken from *E. coli* glycerol stocks using a plasmid purification kit (Macherey-Nagel) wherein DNA was eluted from the columns by 50 μl milliQ water. The peptide-encoding DNA sequences were amplified by two consecutive PCR reactions as previously described[1]. In the first reaction, an equimolar mixture of the five primers NGS_forward 1-5 (5'-TCGTCGGCAGCGTCAGATGTGTATAAGAGACAG$(N)_O$ ATTCTATGCGGCCCAGC-3', O = 0 to 4) was used as the forward primer and an equimolar mixture of the five primers NGS_reverse 1-5 (GTCTCGTGGGCTCGGAGATGTGTATAAGAGACAGG$(N)_O$TTTCA GCGCCAGAACC, O = 0 to 4) was used as the reverse primer. The PCR reaction was prepared as follows. NGS_forward 1-5 (20 nM each, final concentration), NGS_reverse 1-5 (20 nM each, final concentration), dNTP mix (200 μM each, final concentration), 200 ng of phage plasmid DNA as template, 5 μl of 10× Taq buffer and one unit (0.2 μl) of Taq polymerase (New England Biolabs) were used in a 50 μl PCR reaction. The PCR mixture was immediately subjected to thermocycling using the following program: initial denaturation for 2 min at 95°C, 20 cycles of 30 s at 95°C, 60 s at 55°C and 30 s at 68°C, and final elongation for 5 min at 68°C. The amplification efficiency was monitored on a 2% agarose gel (containing 0.005% of ethidium bromide) with a band at around 150-200 base pairs.

In the second PCR reaction, standard Illumina primers containing adapter and index sequences were used as shown below. The PCR reaction was prepared as follows: NGS_PCR2_S505 (100 nM, final concentration), NGS_PCR2_N704 (100 nM, final concentration), dNTP mix (200 μM each, final concentration), 2 μl of reaction mixture of the first PCR (directly used without purification), 5 μL of 10× Taq buffer and one unit (0.2 μL) of Taq polymerase were used in 50 μl of PCR reaction. The PCR was run with the same program as the first PCR. The PCR product was loaded on a 2% agarose gel (containing 0.005% of ethidium bromide and 1 mM guanosine) and the bands with

a size of 200 to 250 base pairs were purified with a gel extraction kit (Qiagen), wherein the DNA was eluted with 20 μl milliQ water. Libraries were subsequently sequenced on a NextSeq 500 instrument (Illumina) according to the manufacturer's instructions. Typically, two million, but at least 0.5 million sequencing reads of peptide were generated for each phage DNA sample. Sequence data was analyzed with MatLab scripts as previously described[2].

Standard Illumina primers:

NGS PCR2 Forward S505	AATGATACGGCGACCACCGAGATCTACACGTAAGGAGTCGTCGGCAGCGTC
NGS PCR2 Forward S506	AATGATACGGCGACCACCGAGATCTACACACTGCATATCGTCGGCAGCGTC
NGS PCR2 Forward S507	AATGATACGGCGACCACCGAGATCTACACAAGGAGTATCGTCGGCAGCGTC
NGS PCR2 Forward S508	AATGATACGGCGACCACCGAGATCTACACCTAAGCCTTCGTCGGCAGCGTC
NGS PCR2 Forward S510	AATGATACGGCGACCACCGAGATCTACACCGTCTAATTCGTCGGCAGCGTC
NGS PCR2 Forward S520	AATGATACGGCGACCACCGAGATCTACACAAGGCTATTCGTCGGCAGCGTC
NGS PCR2 Forward S521	AATGATACGGCGACCACCGAGATCTACACGAGCCTTATCGTCGGCAGCGTC
NGS PCR2 Forward S522	AATGATACGGCGACCACCGAGATCTACACTTATGCGATCGTCGGCAGCGTC
NGS PCR2 Reverse N704	CAAGCAGAAGACGGCATACGAGATGCTCAGGAGTCTCGTGGGCTCGG
NGS PCR2 Reverse N705	CAAGCAGAAGACGGCATACGAGATAGGAGTCCGTCTCGTGGGCTCGG
NGS PCR2 Reverse N706	CAAGCAGAAGACGGCATACGAGATCATGCCTAGTCTCGTGGGCTCGG
NGS PCR2 Reverse N707	CAAGCAGAAGACGGCATACGAGATGTAGAGAGGTCTCGTGGGCTCGG
NGS PCR2 Reverse N714	CAAGCAGAAGACGGCATACGAGATTCATGAGCGTCTCGTGGGCTCGG
NGS PCR2 Reverse N715	CAAGCAGAAGACGGCATACGAGATCCTGAGATGTCTCGTGGGCTCGG
NGS PCR2 Reverse N716	CAAGCAGAAGACGGCATACGAGATTAGCGAGTGTCTCGTGGGCTCGG
NGS PCR2 Reverse N719	CAAGCAGAAGACGGCATACGAGATTACTACGCGTCTCGTGGGCTCGG
NGS PCR2 Reverse N721	CAAGCAGAAGACGGCATACGAGATGCAGCGTAGTCTCGTGGGCTCGG
NGS PCR2 Reverse N727	CAAGCAGAAGACGGCATACGAGATACTGATCGGTCTCGTGGGCTCGG
NGS PCR2 Reverse N728	CAAGCAGAAGACGGCATACGAGATTAGCTGCAGTCTCGTGGGCTCGG
NGS PCR2 Reverse N729	CAAGCAGAAGACGGCATACGAGATGACGTCGAGTCTCGTGGGCTCGG

Synthesis of double-bridged peptides

Peptides were synthesized in house by standard solid-phase peptide synthesis using Fmoc-protected amino acids (0.03 mmol scale). As solid support, Rink amide AM resin was used to obtain peptides with a free N-terminus and an amidated C-terminus. Peptides were cleaved from the resin with a cleavage cocktail (90% TFA, 2.5% H_2O, 2.5% thioanisol, 2.5% phenol, 2.5% 1.2-ethanedithiol) and partially purified by cold ether precipitation. The crude peptide was purified by RP-HPLC (Prep LC 2535 HPLC, Waters) on a C18 column (Sunfire^{TM} prep C18 ODB, 10 μm, 100 Å, 19 × 250 mm, Waters) at a 20 ml min^{-1} flow rate using a linear gradient of the solvents H_2O/0.1% TFA and acetonitrile/0.1% TFA. Purified linear peptide was lyophilized and dissolved in 90% aqueous buffer (60 mM NH_4HCO_3, pH 8.0) and 10% acetonitrile at 1 mM, and reacted with 3 mM of linker reagent for 1 hr at 30°C. The reaction was quenched by adding formic acid (2% [v/v] of the total volume). The chemically modified peptide was lyophilized and purified by RP-HPLC. Peaks corresponding to the three different peptide isomers were collected separately if possible, lyophilized and dissolved in DMSO. The purity was assessed by analytical RP-HPLC (1260 HPLC system, Agilent) equipped with a C18 column (ZORBAX 300SB-C18, 5 μm, 300 Å, 4.6 × 250 mm, Agilent). The mass of purified peptides was confirmed by electrospray ionization mass spectrometry (ESI-MS) in positive ion mode on a single quadrupole liquid chromatography mass spectrometer (LCMS-2020, Shimadzu).

Synthesis of individual double-bridged peptide isomers

Bicyclic peptide isomers with defined pairs of cysteines bridged by chemical linkers were synthesized as previously described[3] with small changes as follows. Peptides were synthesized on Rink amide resin (0.03 mmol scale) as described above wherein the N-terminal Fmoc group was not removed. Two of the cysteines were protected at the side chain with Trt and two with Dpm. The two Trt groups of the cysteines were removed by shaking the resin in 5 ml of TFA:triisopropylsilane:DCM (10:2.5:87.5) in a fritted syringe for 20 min. The solution was removed and the removal of protecting

groups repeated 4 times. After sequential washing with DCM and DMF, 2 ml DMF containing two eq. of cyclization reagent and 2 ml DMF containing 3 eq. of DIPEA were added, and the reaction shaken for 1 hr at room temperature. The reaction solution was removed and the resin was washed with DMF (5 ml × 3). The N-terminal Fmoc protecting group was removed by adding twice 3 ml of 20% piperidine in DMF for 5 min and shaking. The resin was washed with DMF (5 ml × 3) and subjected to global deprotection in 5 ml of the cleavage mixture (91.5% TFA, 2.5% H_2O, 2.5% thioanisol, 1% triisopropylsilane, 2.5% phenol) for 12 hrs. The resin was filtered and peptide was precipitated and washed by cold ether. The crude peptide was lyophilized, dissolved in 90% aqueous buffer (60 mM NH_4HCO_3, pH 8.0) and 10% acetonitrile to reach a concentration of 1 mM, and reacted with 1.5 mM of cyclization reagent for 1 hr at 30°C (added in 1/10 volume of ACN at 15 mM). The reaction was quenched by adding formic acid to 2% (v/v) of total volume. The peptide was lyophilized and purified by RP-HPLC.

Protease inhibition assay

Inhibition constants (K_i) were determined by measuring the residual activities of protease in the presence of different dilutions of inhibitor (2-fold dilutions, ranging from 10 μM to 0.2 nM final concentration) using chromogenic or fluorogenic peptide substrates. Activities were measured at 25°C in buffer containing 10 mM Tris-Cl, pH 7.4, 150 mM NaCl, 10 mM $MgCl_2$, 1 mM $CaCl_2$, 0.1% (w/v) BSA and 0.01% (v/v) Triton-X100 by monitoring the change in 405 nm absorption (for pNA substrate) or fluorescence intensity (excitation at 367 nm, emission at 468 nm, for AMC substrates) over one hour using a Tecan Infinite M200 Pro plate reader. For measuring FXIa inhibition, Pyr-Pro-Arg-pNA (400 μM final concentration) was added to buffer containing FXIa at 0.5 nM in the presence or absence of peptides. Hydrolysis of the substrate resulted in the release of p-nitroaniline, which was monitored by measuring the increase in absorbance at 405 nm. The rate of absorbance change is proportional to enzyme activity. The IC_{50} values were determined by fitting sigmoidal curves to the data using the following four-parameter logistic equation:

$$Y = \frac{100}{1 + 10^{(\mathrm{Log}IC_{50} - X)p}}$$

Wherein Y is the residual activity (%) of protease, X is the logarithm of peptide concentration, IC_{50} is the concentration of inhibitor that produces 50% inhibition, and p is the Hill coefficient. The K_i values were calculated based on the IC_{50}s using the Cheng-Prusoff equation:

$$K_i = \frac{IC_{50}}{1 + \frac{[S]_0}{K_m}}$$

Wherein $[S]_0$ is the initial concentration of substrate, and K_m is the Michaelis-Menten constant for the enzyme and substrate pair. The K_m of FXIa for Pyr-Pro-Arg-pNA was determined to be 255 ± 14 μM.

The selectivity of the double-bridged peptides was assessed by testing the inhibition of a panel of human proteases that are structurally and/or functionally related to FXIa. The following concentrations of enzyme were used: 0.1 nM plasma kallikrein, 2 nM factor XIIa, 2 nM thrombin, 1.5 nM uPA, 7.5 nM tPA, 2.5 nM plasmin, 6 nM factor Xa, 0.05 nM trypsin. The following fluorogenic substrates were used at 50 μM final concentration: Z-Phe-Arg-AMC for plasma kallikrein, Z-Gly-Gly-Arg-AMC for factor XIIa, thrombin, trypsin, uPA and tPA, H-D-Val-Leu-Lys-AMC for plasmin, D-Phe-Pro-Arg-ANSNH-C_4H_9 for factor Xa.

Measurement of aPTT

Activated partial thromboplastin time (aPTT) was determined in human or mouse plasma using a temperature-controlled Stago STart4 Coagulation analyzer (Diagnostica). Human single donor plasma was used (Innovative Research). To a volume of 100 μl of citrated human plasma, 10 μl double-bridged peptide (in buffer 50 mM Tris-Cl pH7.4, 150 mM NaCl, 5 mg/mL BSA) was added. 100 μl of the above solution was transferred to the cuvette (Stago, CAT#38876) with a steel ball (Stago,

CAT#26441) and 100 μl of Pathromtin SL (silicon dioxide particles, plant phospholipids in HEPES buffer system, Siemens) was added, and incubated for 2 min at 37°C. The coagulation was triggered by addition of 100 μl pre-warmed (37°C) $CaCl_2$ solution (25 mM, Siemens). Coagulation was monitored by measuring an electromagnetically induced movement of a steel ball in the plasma, and the time until the ball stopped moving was recorded as coagulation time. For aPTT measurements in mouse, rabbit, and rat plasma, 100 µl of plasma was placed into the cuvette, 100 μl of Dade Actin (Cephalin, Ellagic acid in HEPES buffer system; Siemens) was added and incubated for three minutes at 37°C in the device before coagulation was triggered by addition of 100 µl $CaCl_2$ solution.

Expression and purification of FXI catalytic domain

Recombinant human FXI catalytic domain (D357 to V607) with two point mutations (N473G, T475G), an N-terminal addition of MDDDD and C-terminal 6×His-tag was cloned as previously described[4] with small changes. The DNA coding these elements was synthesized (Eurofin) and inserted into the bacterial expression vector pET22b (Novagen) using the restriction enzymes *Nde*I and *Eco*RI, the vector transformed into electrocompetent DH5α *E. Coli* cells, and the cells plated on ampicillin selective 2YT agar plates. The DNA coding for the FXI catalytic domain was sequenced to verify the correctness of the sequence, and plasmid was transformed into electrocompetent BL21 Star™ (DE3) *E. coli* cells. The cells were grown in 800 ml 2YT in 2.5 L shaking flasks (200 rpm) at 37°C until the logarithmic growth phase was reached. Expression was induced with 0.4 mM IPTG at 30°C and cells were harvested 12 hrs later by centrifugation. The catalytic domain of FXI was expressed as inclusion bodies in the conditions described above. Inclusion bodies were isolated as follows. Cell pellets of around 10 g were suspended in 100 ml of lysis buffer (50 mM Tris-Cl, pH 8.0, 100 mM NaCl, 1 mM DTT, and 1% Triton-X 100) and lysed by sonication (Vibra-Cell™). The lysate suspension was clarified by centrifugation at 10,000 × *g* for 30 min at 4°C, the pellets were washed twice with 20 ml lysis buffer under sonication and solubilized with

2 ml dissolving buffer (50 mM Tris-Cl, pH 8.5, 6 M guanidine HCl, and 10 mM DTT) at room temperature for 1 hr. Solubilized protein was refolded at a final concentration of 0.5 mg ml^{-1} by rapid dilution into 100 ml refolding buffer (100 mM CAPSO, pH 9.5, 0.9 M arginine, and 0.3:0.03 mM reduced/oxidized glutathione) under vigorous stirring at room temperature, and left at 4°C overnight. Refolded protein was concentrated with a Vivaspin® 20 filter (molecular weight cut off of 10 kDa) and exchanged into buffer A (50 mM Tris-Cl, pH 8.0, 500 mM NaCl) using a HiPrep 26/10 Desalting column (GE Healthcare). Thrombin (1000 units; Sigma, SRP6555-10 KU) was added, and the mixture was incubated for 30 min at 37°C to convert the FXI catalytic domain into the active form (FXIa catalytic domain). The protein was loaded onto a nickel affinity column (GE Healthcare) and eluted with buffer A and applying a gradient of imidazole from 10 to 250 mM. Fractions containing FXIa catalytic domain were identified by SDS-PAGE, pooled and loaded onto a 5 ml benzamidine Sepharose column (GE Healthcare) equilibrated with 50 mM Tris, pH 7.4, 1 M NaCl. The column was washed with the same buffer. FXIa catalytic domain bound to benzamidine was eluted in the same buffer supplemented with 40 mM benzamidine sulfate.

Synthetic DNA cloned into pET22b (underlined are the restriction sites for cloning):

ATTCTATGCGGCCCAGC<u>CATATG</u>GATGACGATGACAAAATGGATAATGAATGCAC
CACCAAAATCAAGCCTCGTATTGTTGGTGGCACCGCAAGCGTTCGTGGTGAATG
GCCGTGGCAGGTTACCCTGCATACCACCAGTCCGACACAGCGTCATCTGTGTG
GTGGTAGCATTATTGGTAATCAGTGGATTCTGACCGCAGCGCATTGTTTTTATGGT
GTTGAAAGCCCGAAAATTCTGCGTGTTTATAGCGGTATTCTGAACCAGAGCGAAA
TCAAAGAAGATACCAGCTTTTTTGGCGTGCAAGAAATCATCATCCACGACCAGTA
TAAAATGGCAGAAAGCGGTTATGATATTGCCCTGCTGAAACTGGAAACCACCGTT
GGTTATGGTGATAGCCAGCGTCCGATTTGTCTGCCGAGCAAAGGTGATCGTAAT
GTGATTTATACCGATTGTTGGGTTACCGGTTGGGGTTATCGTAAACTGCGTGATAA
AATTCAGAACACCCTGCAGAAAGCAAAAATTCCGCTGGTTACCAATGAAGAATGC
CAGAAACGTTATCGCGGTCATAAAATCACCCATAAAATGATTTGTGCCGGTTATCG

TGAAGGTGGTAAAGATGCATGTAAAGGTGATAGCGGTGGTCCGCTGAGCTGTAA
ACATAATGAAGTTTGGCATCTGGTTGGTATTACCAGCTGGGGTGAAGGTTGTGCA
CAGCGTGAACGTCCGGGTGTTTATACCAATGTTGTTGAATATGTGGACTGGATCC
TGGAAAAAACCCAGGCAGTTCATCATCACCATCATCATTAAGAATTCGGTTCTGG
CGCTGAAA

Co-crystallization of FXIa and double-bridged peptides

Crystals of FXIa catalytic domain were grown at 18°C by using the hanging-drop vapor diffusion method. The protein (10 mg ml^{-1}) was mixed with an equal volume of reservoir solution containing 200 mM $(NH_4)_2SO_4$, 25% PEG4000, and 100 mM NaOAc, pH 4.6. Crystals of FXIa catalytic domain/peptide complex were prepared by co-crystallization of protein (10 mg ml^{-1}, 0.36 mM) and peptide (1 mM) in the same condition and seeded with the native crystals. Crystals grown up in two days were cryoprotected in reservoir solution containing 20% glycerol and frozen in liquid nitrogen for mounting prior to X-ray diffraction.

X-ray structure determination

Data for FXIa crystals in complex with peptides F19 and F21 was collected at the beamline PXIII of the Swiss Light Source at the Paul Scherrer Institute (SLS, Villigen, Switzerland) at a wavelength of 1.0 Å. Raw data were processed with the program XDS[5]. The structures were solved by molecular replacement using Phaser using the atomic coordinates of FXIa catalytic domain (PDBID: 4TY6) as a search model. The models were subjected to iterative rounds of re-building and refinement in Coot and REFMAC5, part of Phenix software suite[6]. The data collection and refinement statistics are summarized in Supplementary Table 1. The atomic coordinates and the structure factors were deposited in the Protein Data Bank. PDB deposition numbers for double-bridged peptides F19 and F21 complexed to FXIa catalytic domain are 6TWB, and 6TWC, respectively. Molecular graphic figures were generated using PyMOL[7].

Circular dichroism spectroscopy

Circular dichroism measurements were performed using a 200 μM solution of peptide in 20 mM phosphate buffer, pH 7.4. Optionally, the solution contained 40% (v/v) TFE. Spectra were measured from 250 nm to 190 nm on a J-815 Spectropolarimeter (Jasco).

NMR spectroscopy

For nuclear magnetic resonance (NMR) spectroscopy, lyophilized F19 was dissolved to a final concentration of 4 mM in either 90% H_2O/10% D_2O (pH 4.0) or 90% sodium phosphate buffer (20 mM, pH 7.4)/10% D_2O. All presented data corresponds to pH 4, as at pH 7 the $^3J_{HNHA}$ couplings are masked by line broadening in the amide region of ^1H spectra, where the coupling is measured. ^1H,^{13}C HSQC spectra are superimposable at both pH indicating essentially the same degree of (un)structuring. All NMR experiments were carried out in a Bruker 800 MHz spectrometer equipped with a CPTC ^1H,^{13}C,^{15}N 5 mm cryoprobe. Assignments were achieved through a combination of ^1H-^1H TOCSY (60 ms spin lock), ^1H-^1H NOESY (250 ms mixing time), natural abundance ^1H-^{13}C HSQC and natural abundance ^1H-^{15}N HSQC, using the standard Bruker pulse sequences dipsi2esgpph, noesyesgpph, hsqcetgp and hsqcetfpf3gpsi, respectively. Spectra were processed with TopSpin and analyzed with CARA.

Cloning, expression and purification of IL-23R

DNA encoding the extracellular domain of human IL-23R (residues Met1-Glu317) was cloned into pEXPR-IBA42 for the expression of poly-histidine tagged IL-23R in mammalian cells. The vector contains a BM40 leader sequence for secretion of the protein into the medium. The DNA was cloned in two steps: first, the entire IL-23R gene (containing the intracellular region; synthetic gene is shown below) was cloned into the vector pEXPR-IBA42 using the restriction enzymes *Nhe*I and *Xho*I. Second, the region of the vector and the extracellular domain of IL-23R was amplified by whole-plasmid

DNA using the primers Jun-forward (CCTTGGCTCGAGGTCGACCTGCAGGGGGAC) and Jun-backward (GGAACCCTCGAGTCAGTGATGGTGATGGTGATGCCTTCCCT CGATTTCAGGTGTTTTATGAAAAAACAGTGAAC), the product digested by *Xho*I, and the DNA circularized by ligation.

The protein was expressed by transient transfection of HEK293 cells (Freestyle™ 293-F) in a 1-liter suspension culture as described in the following. Suspension-adapted HEK 293 cells were maintained in serum-free ExCell 293 medium (SAFC Biosciences) with 4 mM glutamine with inoculation at 0.3 x 10^6 cells/ml as described[8]. On the day before transfection, cells were inoculated into fresh medium at a density of 1 × 10^6 cells/ml. The next day, 1 × 10^9 cells were harvested by centrifugation at 1,200 rpm for 5 min and resuspended at a density of 2 × 10^7 cells/ml in 50 ml of RPMI 1640 medium with 0.1% pluronic F68 (SAFC Biosciences) in a TubeSpin® bioreactor 600 tube (TPP)[9]. Plasmid DNA (1.5 mg) and linear 25 kDa polyethylenimine (3 mg; 1 mg/ml in H_2O; Polysciences) were sequentially added and mixed. The culture was agitated by orbital shaking at 180 rpm in an ISF-4-W incubator (Kühner AG) at 37°C in the presence of 5% CO_2. After 60 min, the transfected culture was transferred to a 5-L glass bottle containing 950 ml of FreeStyle 293 medium (Life Technologies) with 4 mM glutamine and 3.75 mM valproic acid (500 mM in H_2O) (SAFC Biosciences)[10]. The culture was transferred to an incubator shaker at 37°C with 5% CO_2 with agitation at 120 rpm. At 7 d post-transfection, the cell culture medium was recovered by centrifugation at 2,500 rpm for 20 min and filtered through a 0.22 μm membrane.

IL-23R was purified from the culture supernatant by Ni-NTA affinity chromatography. Eluted protein was further purified by size-exclusion chromatography on a Superdex75 10/300 GL (GE healthcare) column using 20 mM HEPES (pH 7.4) and 150 mM NaCl as buffer.

Amino acid sequence of expressed protein, including the BM40 leader (underlined), the dipeptide Ala-Ser following the leader, the human IL-23R extra cellular domain, a linker (Ile-Glu-Gly-Arg) and a poly-histidine tag:

MRAWIFFLLCLAGRALAASMNQVTIQWDAVIALYILFSWCHGGITNINCSGHIWVEPA
TIFKMGMNISIYCQAAIKNCQPRKLHFYKNGIKERFQITRINKTTARLWYKNFLEPHAS
MYCTAECPKHFQETLICGKDISSGYPPDIPDEVTCVIYEYSGNMTCTWNAGKLTYIDT
KYVVHVKSLETEEEQQYLTSSYINISTDSLQGGKKYLVWVQAANALGMEESKQLQIH
LDDIVIPSAAVISRAETINATVPKTIIYWDSQTTIEKVSCEMRYKATTNQTWNVKEFDT
NFTYVQQSEFYLEPNIKYVFQVRCQETGKRYWQPWSSLFFHKTPEIEGRHHHHHH

Synthetic DNA cloned into pEXPR-IBA42 (underlined are the restriction sites for cloning):

5'-ATTCTATGCGGCCCAGCGCTAGCATGAATCAGGTCACTATTCAATGGGATGCAGTAATAGCCCT
TTACATACTCTTCAGCTGGTGTCATGGAGGAATTACAAATATAAACTGCTCTGGCCACATCTGGGTAG
AACCAGCCACAATTTTTAAGATGGGTATGAATATCTCTATATATTGCCAAGCAGCAATTAAGAACTGCC
AACCAAGGAAACTTCATTTTTATAAAAATGGCATCAAAGAAAGATTTCAAATCACAAGGATTAATAAAA
CAACAGCTCGGCTTTGGTATAAAAACTTTCTGGAACCACATGCTTCTATGTACTGCACTGCTGAATGT
CCCAAACATTTTCAAGAGACACTGATATGTGGAAAAGACATTTCTTCTGGATATCCGCCAGATATTCC
TGATGAAGTAACCTGTGTCATTTATGAATATTCAGGCAACATGACTTGCACCTGGAATGCTGGGAAGC
TCACCTACATAGACACAAAATACGTGGTACATGTGAAGAGTTTAGAGACAGAAGAAGAGCAACAGTA
TCTCACCTCAAGCTATATTAACATCTCCACTGATTCATTACAAGGTGGCAAGAAGTACTTGGTTTGGG
TCCAAGCAGCAAACGCACTAGGCATGGAAGAGTCAAAACAACTGCAAATTCACCTGGATGATATAGT
GATACCTTCTGCAGCCGTCATTTCCAGGGCTGAGACTATAAATGCTACAGTGCCCAAGACCATAATTT
ATTGGGATAGTCAAACAACAATTGAAAAGGTTTCCTGTGAAATGAGATACAAGGCTACAACAAACCAA
ACTTGGAATGTTAAAGAATTTGACACCAATTTTACATATGTGCAACAGTCAGAATTCTACTTGGAGCCA
AACATTAAGTACGTATTTCAAGTGAGATGTCAAGAAACAGGCAAAAGGTACTGGCAGCCTTGGAGTT
CACTGTTTTTTCATAAAACACCTGAAACAGTTCCCCAGGTCACATCAAAAGCATTCCAACATGACACA
TGGAATTCTGGGCTAACAGTTGCTTCCATCTCTACAGGGCACCTTACTTCTGACAACAGAGGAGACA
TTGGACTTTTATTGGGAATGATCGTCTTTGCTGTTATGTTGTCAATTCTTTCTTTGATTGGGATATTTAA

CAGATCATTCCGAACTGGGATTAAAAGAAGGATCTTATTGTTAATACCAAAGTGGCTTTATGAAGATAT

TCCTAATATGAAAAACAGCAATGTTGTGAAAATGCTACAGGAAAATAGTGAACTTATGAATAATAATTC

CAGTGAGCAGGTCCTATATGTTGATCCCATGATTACAGAGATAAAAGAAATCTTCATCCCAGAACACA

AGCCTACAGACTACAAGAAGGAGAATACAGGACCCCTGGAGACAAGAGACTACCCGCAAAACTCGC

TATTCGACAATACTACAGTTGTATATATTCCTGATCTCAACACTGGATATAAACCCCAAATTTCAAATTTT

CTGCCTGAGGGAAGCCATCTCAGCAATAATAATGAAATTACTTCCTTAACACTTAAACCACCAGTTGA

TTCCTTAGACTCAGGAAATAATCCCAGGTTACAAAAGCATCCTAATTTTGCTTTTTCTGTTTCAAGTGT

GAATTCACTAAGCAACACAATATTTCTTGGAGAATTAAGCCTCATATTAAATCAAGGAGAATGCAGTTC

TCCTGACATACAAAACTCAGTAGAGGAGGAAACCACCATGCTTTTGGAAAATGATTCACCCAGTGAA

ACTATTCCAGAACAGACCCTGCTTCCTGATGAATTTGTCTCCTGTTTGGGGATCGTGAATGAGGAGT

TGCCATCTATTAATACTTATTTTCCACAAAATATTTTGGAAAGCCACTTCAATAGGATTTCACTCTTGGA

AAAGATCGAGGGAAGGCATCACCATCACCATCACTGA<u>CTCGAG</u>GGTTCTGGCGCTGAAA-3'

Measuring peptide binding by SPR

Binding kinetics and dissociation constants of double-bridged peptides to immobilized IL-23R were analyzed by surface plasmon resonance (SPR). The experiments were performed using a Biacore^{TM} 8K instrument (GE Healthcare). IL-23R (3.3 μg/mL) was dissolved in 10 mM acetate buffer (pH 5.5) and immobilized on a CM5 series S chip by standard amine coupling method in running buffer (10 mM HEPES pH 7.4, 150 mM NaCl, 3 mM EDTA, and 0.005% (v/v) Tween-20). Typical immobilization level was 2000 to 3000 resonance units (RUs). The reference cell was treated the same way without IL-23R. For the measurement of binding kinetics and dissociation constants, five serial dilutions (2-fold) of peptides were prepared in running buffer (10 mM HEPES pH 7.4, 150 mM NaCl, 3 mM EDTA, 0.005% (v/v) Tween-20, and 5% (v/v) DMSO) and analyzed in single cycle kinetics mode with the contact and dissociation times of 60 s and 120 s, respectively.

References

1. Villequey, C., Kong, X. D. & Heinis, C. Bypassing bacterial infection in phage display by sequencing DNA released from phage particles. *Protein Eng. Des. Sel.* **30**, 761–768 (2017).

2. Rentero Rebollo, I., Sabisz, M., Baeriswyl, V. & Heinis, C. Identification of target-binding peptide motifs by high-throughput sequencing of phage-selected peptides. *Nucleic Acids Res.* **42**, e169 (2014).

3. Kale, S. S. *et al.* Cyclization of peptides with two chemical bridges affords large scaffold diversities. *Nat. Chem.* **10**, 715–723 (2018).

4. Hangeland, J. J. *et al.* Phenylimidazoles as potent and selective inhibitors of coagulation factor XIa with in vivo antithrombotic activity. *J. Med. Chem.* (2014). doi:10.1021/jm5010607

5. Kabsch, W. *et al. XDS*. *Acta Crystallogr. Sect. D Biol. Crystallogr.* (2010). doi:10.1107/S0907444909047337

6. Adams, P. D. *et al.* PHENIX: A comprehensive Python-based system for macromolecular structure solution. *Acta Crystallogr. Sect. D Biol. Crystallogr.* (2010). doi:10.1107/S0907444909052925

7. Delano, W. L. The PyMOL Molecular Graphics System. *Schrodinger* (2002). doi:citeulike-article-id:240061

8. Muller, N., Girard, P., Hacker, D. L., Jordan, M. & Wurm, F. M. Orbital shaker technology for the cultivation of mammalian cells in suspension. *Biotechnol. Bioeng.* **89**, 400–406 (2005).

9. Backliwal, G., Hildinger, M., Hasija, V. & Wurm, F. M. High-density transfection with HEK-293 cells allows doubling of transient titers and removes need for a priori DNA complex formation with PEI. *Biotechnol. Bioeng.* **99**, 721–727 (2008).

10. Backliwal, G. *et al.* Valproic acid: A viable alternative to sodium butyrate for enhancing protein expression in mammalian cell cultures. *Biotechnol. Bioeng.*

101, 182–189 (2008).

Supplementary Tables

Supplementary Table 1. Data collection and refinement statistics for FXIa catalytic domain complexed with double-bridged peptides F19 (PDBID: 6TWB) and F21 (PDBID: 6TWC).

	FXIa CAT-F19[a]	FXIa CAT-F21[b]
Data collection		
Space group	$P3_221$	$P3_221$
Cell dimensions		
a, *b*, *c* (Å)	77.5, 77.5, 116.5	76.2, 76.2, 117.1
α, β, γ (°)	90, 90, 120	90, 90, 120
Resolution (Å)	44.0 – 2.91 (3.08 – 2.91)*	43.8 – 2.86 (3.03 – 2.86)
R_{meas}	0.18 (0.82)	0.13 (1.02)
$I / \sigma I$	13.3 (2.7)	22.3 (3.3)
Completeness (%)	99.9 (99.3)	99.6 (98.7)
Redundancy	10.7 (9.4)	12.3 (11.5)
Refinement		
Resolution (Å)	44.0 – 2.91	43.8 – 2.86
No. reflections	9318	9461
R_{work} / R_{free}	0.179 / 0.241	0.213 / 0.259
No. atoms		
Protein	1943	1951
Ligand/ion	84	103
Water	10	0
B-factors		
Protein	56.2	67.9
Ligand/ion	53.1	67.2
Water	43.0	
R.m.s. deviations		
Bond lengths (Å)	0.009	0.009
Bond angles (°)	1.029	1.206

[a,b] One crystal used for the data collection of each structure.

[c] Values in parentheses are for highest-resolution shell.

Supplementary Table 2. The surface and interface area of FXIa catalytic domain and double-bridged peptides calculated using the PDBePISA web server.

Peptide	Protein (Å^2)	Peptide (Å^2)	Interface area (Å^2)
F19	11375	1290	649.3
F21	11421	1480	727.5

Supplementary Table 3. NMR Spectroscopy data. Backbone HN, HA, N, CA and CB assignments (chemical shifts in ppm), ^{3}J HN-HA couplings (Hz), selected H-H NOE strengths, and analysis of chemical shifts with the CSI 3.0 server.

aa	Raw chemical shifts as assigned				Random coil shifts for canonical amino acids				CSI 3.0	Strength of H-H NOEs				^{3}J HN-HA
										sequential		expected in helix		
	HN	HA	N	CA	CB	CA	CB	dCA-dCB	output	$d_{NN}(i,i+1)$	$d_{aN}(i,i+1)$	$d_{aN}(i,i+3)$	$d_{aN}(i,i+4)$	(Hz)
C*1	NE	UI	NE	UI	UI	58.8	28.6	NA	NA	NA	NA	NA	NA	NE
V2	8.21	3.97	124.8	60.1	29.4	63	31.7	-0.32	C	|||	||	0	0	6.87
N3	7.9	UI	117.6	UI	36.2	53.6	39	NA	C			NA	NA	NA	8.38
I4	8.27	4.16	122.5	60.1	35.6	62.6	37.5	0.63	C	0	|||	0	0	7
M5	8.33	4.38	120.2	54.1	29.1	56.6	32.8	-1.17	C	|||	|||	0	0	6.46
C6	8.02	UI	116.3	UI	31.4	58.8	28.6	NA	B	||	0	NA	NA	8.56
C7	7.95	4.14	120.9	55.6	32.8	58.8	28.6	7.38*	C	|||		NA	NA	4.46*
R8	8.26	4.36	116.1	52.7	26.9	56.3	30.3	0.21	C	|||	||	NA	NA	8.9
C9	7.65	UI	120.3	UI	32.9	58.8	28.6	NA	B	NA	NA	NA	NA	7.88
P10	NE	4.31	UI	60.8	29.6	62.9	31.7	-0.03	C	NA	NA	NA	NA	NE

*For Cys7, CSI and ^{3}J values seem indicative of helical secondary structure, but being a non-canonical cysteine, this is hard to ascertain (especially regarding the ^{13}C shifts).

NA = not applicable, because one or more resonances are non-existent (NE) or remain unidentified (UI)

dCA - dCB = (CA observed - CA for random coil) - (CB observed - CB for random coil) is a calibration-independent proxy for secondary structure, positive for alpha helix propensity and negative for sheet propensity (absolute value > 1.5 ppm for well-defined secondary structures)

^{3}J HN-HA coupling is < 6 Hz for helical structures and >8 for beta sheets

CSI 3.0 was calculated with the online server at http://csi3.wishartlab.com/cgi-bin/index.php. In CSI's output, C stands for coiled coil and B for β-sheet structure

NOE strengths are indicated qualitatively from 0 (absent crosspeak) to strong (three bars, |||, as observed for intraresidue HN-HA pairs). Notations $d_{NN}(i,i+1)$, $d_{aN}(i,i+1)$, $d_{aN}(i,i+3)$ and $d_{aN}(i,i+4)$ stand for short distances (i.e. strong NOEs expected) between HN and HA resonances of residues separated by 1, 3 or 4 positions in the peptide's sequence (all expected in helical structures).

Supplementary Figures

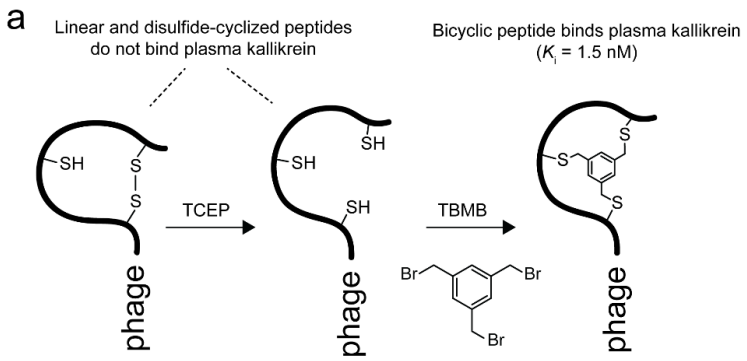

Peptide sequence of PK15: ACSDRFRNCPADEALCG

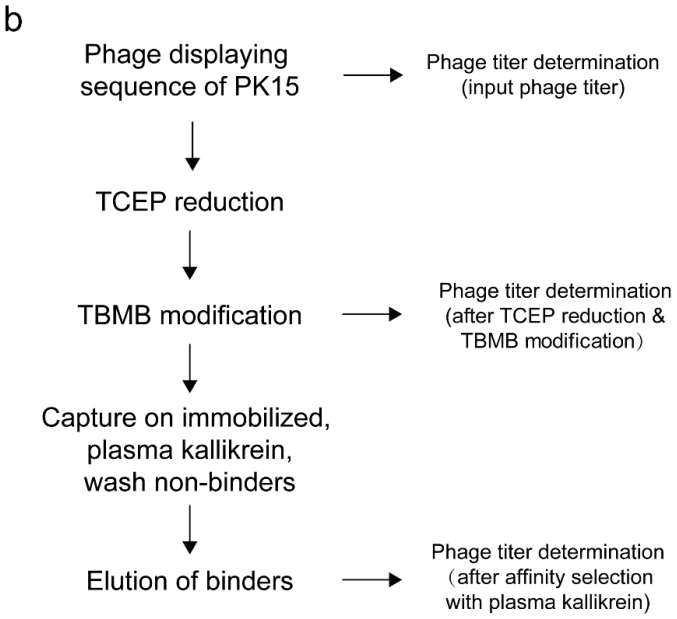

Supplementary Figure 1 Strategy to quantify peptide cyclization efficiency on the tip of phage using the peptide PK15. a, Cyclization of peptide PK15 displayed on phage with TBMB. Only peptide correctly cyclized with TBMB binds to plasma kallikrein. Linear peptide or disulfide-cyclized side products do not bind with high affinity. **b**, Procedure applied to assess integrity of phage through infectivity measurement and cyclization of peptide through capture of PK15 on immobilized plasma kallikrein.

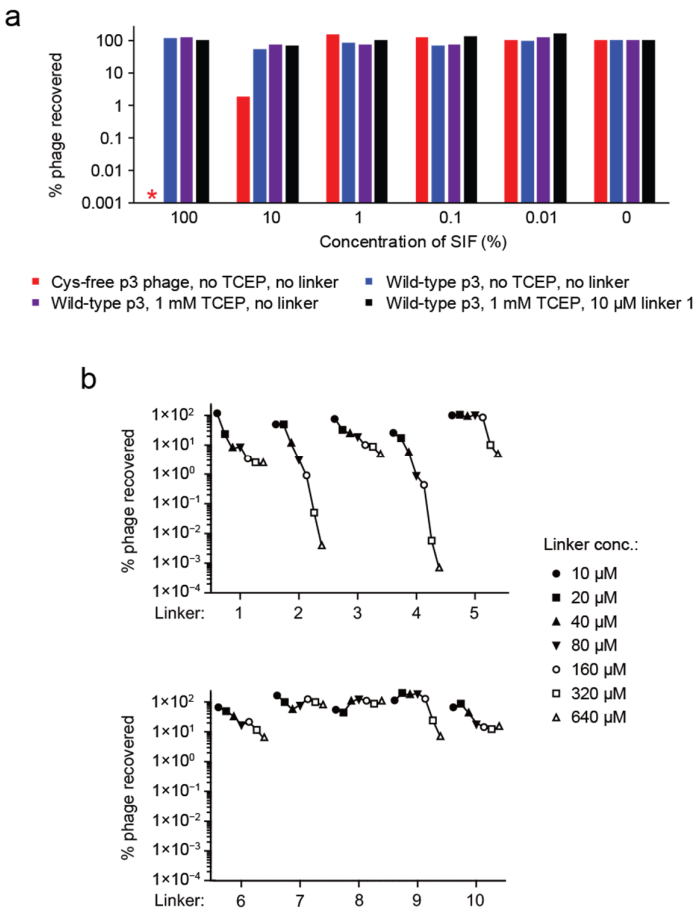

Supplementary Figure 2 Effect of simulated intestinal fluid (SIF) and cyclization reagent concentration on infectivity of wild-type phage. a, Wild-type or cysteine-free p3 phage were modified and treated with pancreatin as indicated. The percentages of phage remaining infective after exposure to the various concentrations of pancreatin (indicated in % SIF) are indicated. * no colony observed, < 0.001% of infectivity recovery. **b,** TCEP-treated wild-type phage were exposed to different concentrations of the reagents **1** to **10** shown in Fig. 1d and the number of phage that remained functional assessed by infection of bacteria. Concentrations of 20 µM (**1**, **2** and **4**) and 40 µM (**3**, **5**, **6**, **7**, **8**, **9**, **10**) reduced the number of functional phage less than 10-fold and were considered suited for wild-type phage peptide double-bridging.

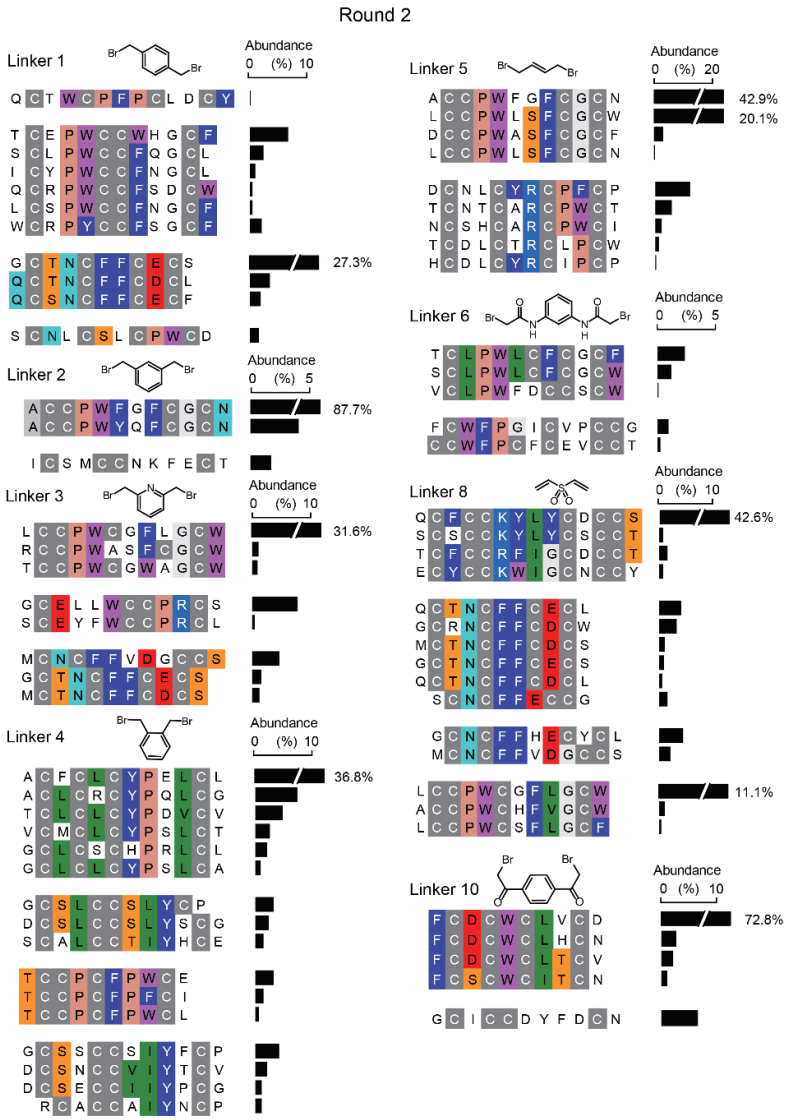

Supplementary Figure 3 Sequences of peptides enriched in phage selection rounds 2 and 3 using reagents 1-6, 8 and 10. Peptides with similar sequences are aligned in groups and amino acid similarities are highlighted in color. For peptides that represented more than 2, 5, 10 or 20% of the sequenced population, the abundance is indicated with a number. Peptides isolated with cyclization reagent **9** did not show sequence similarities and are not shown, and those isolated in round 2 with reagent **7** are shown in Fig. 2.

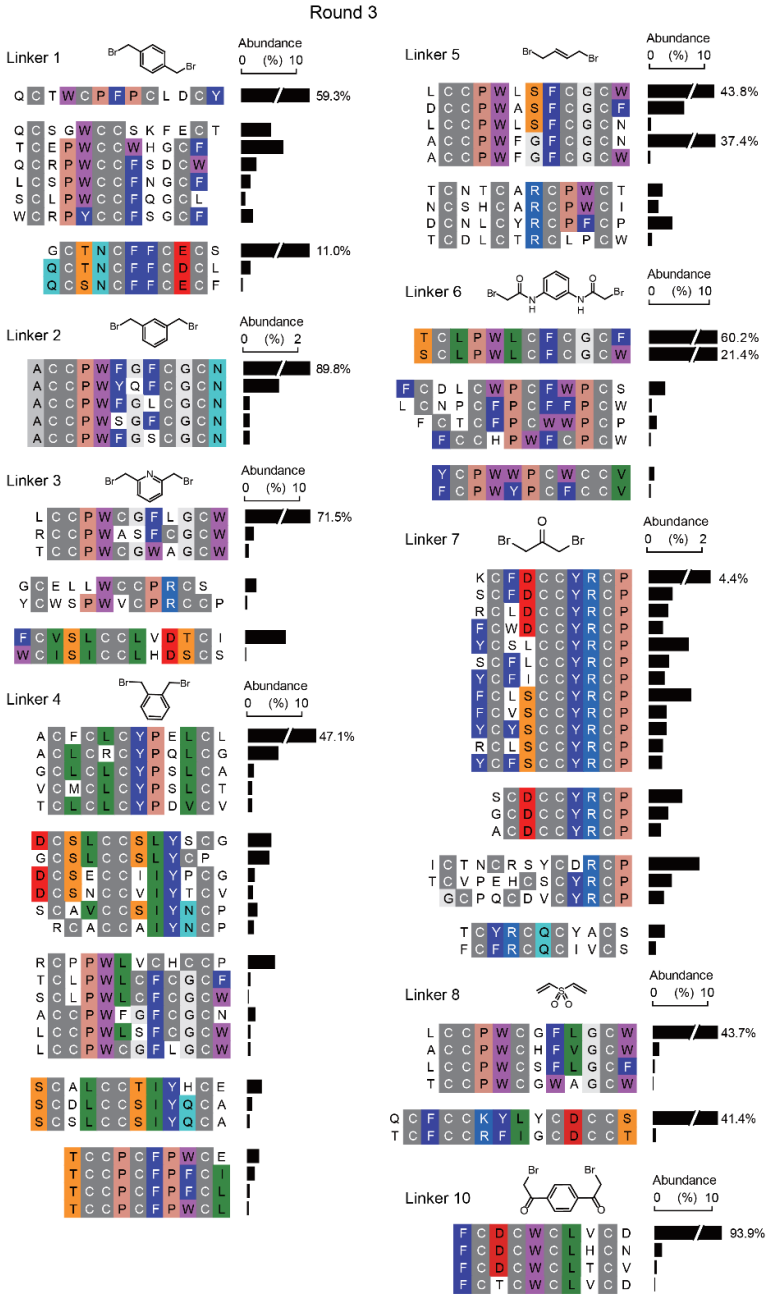

Supplementary Figure 3 Continued

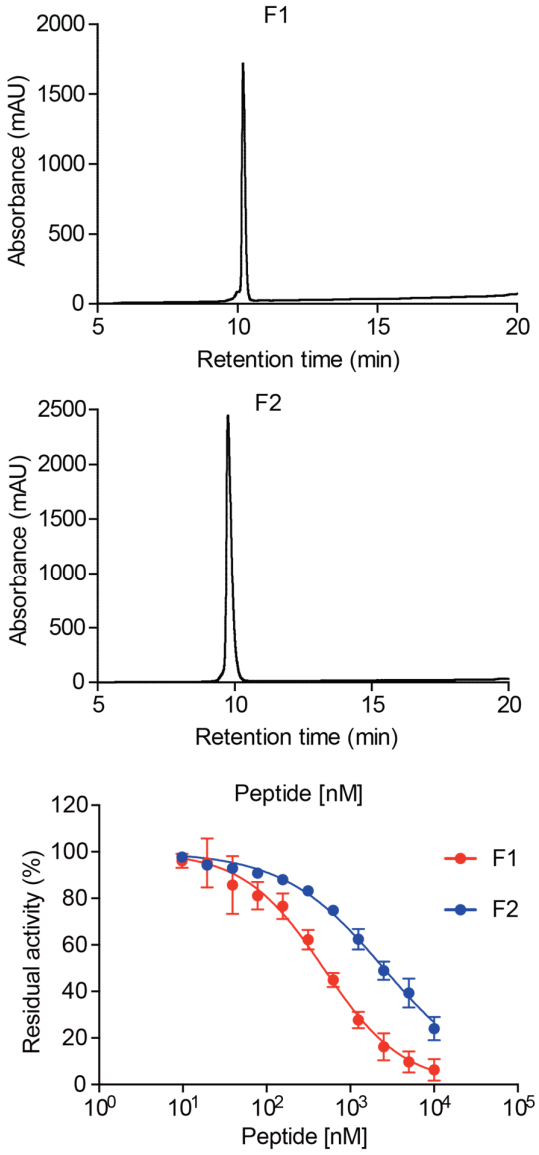

Supplementary Figure 4 Activity of two peptides strongly enriched in selection round 2 with reagent 7. The peptides F1 and F2 were cyclized with reagent **7**, the three isomers of each separated by HPLC and the inhibition of FXIa tested in an activity assay using a chromogenic substrate. The upper two panels show the analytical HPLC chromatograms of the active isomers of F1 and F2. The experiment was performed one time. The bottom panel shows the inhibition of FXIa at increasing double-bridged peptide concentrations. Means and SD of four measurements are shown.

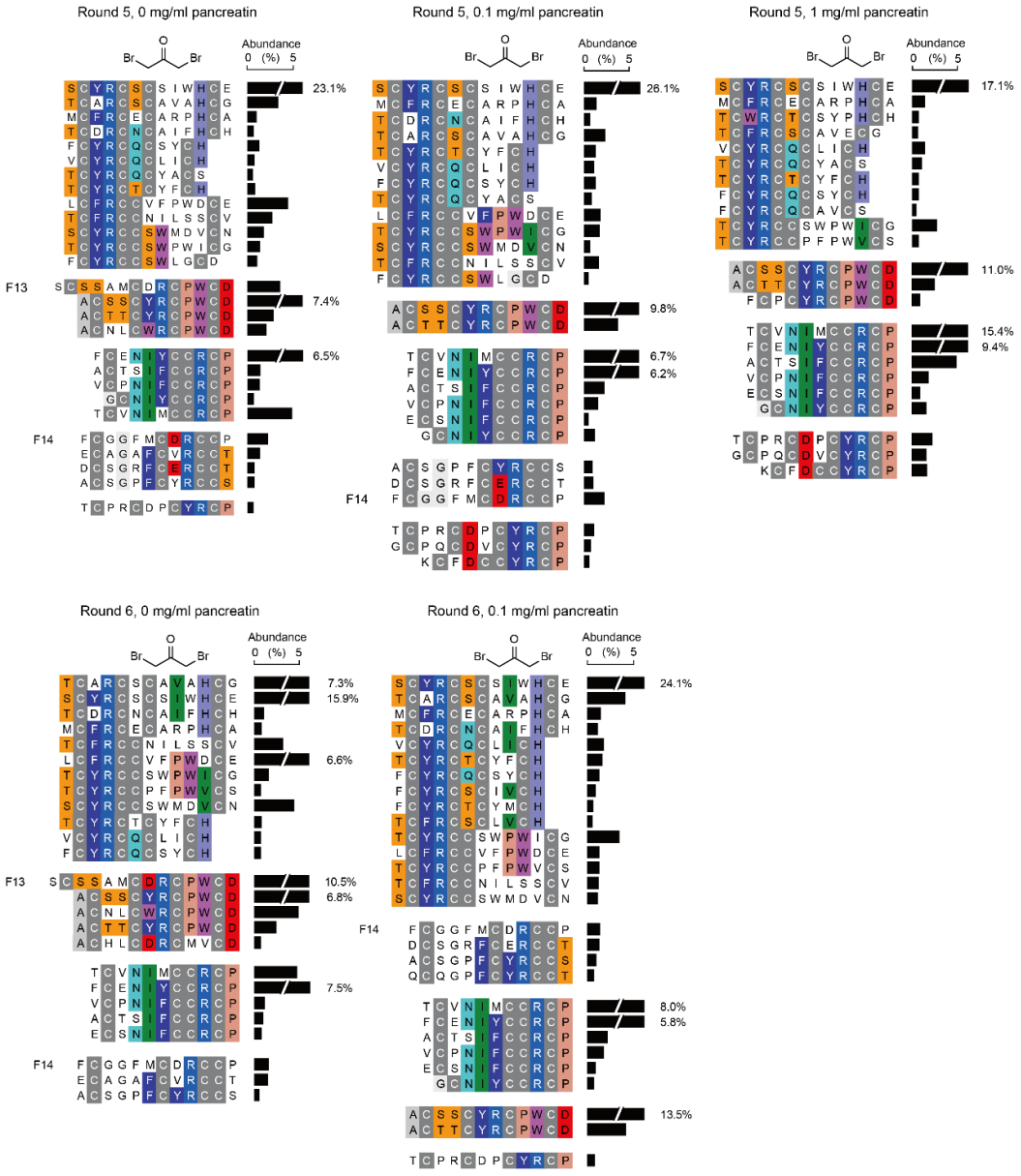

Supplementary Figure 5 Sequences of peptides isolated in phage selection rounds 5 and 6 using reagent 7 and different proteolytic pressures. Peptides with similar sequences are aligned in groups and amino acid similarities are highlighted in color. Peptides that were synthesized and characterized are labeled with a name.

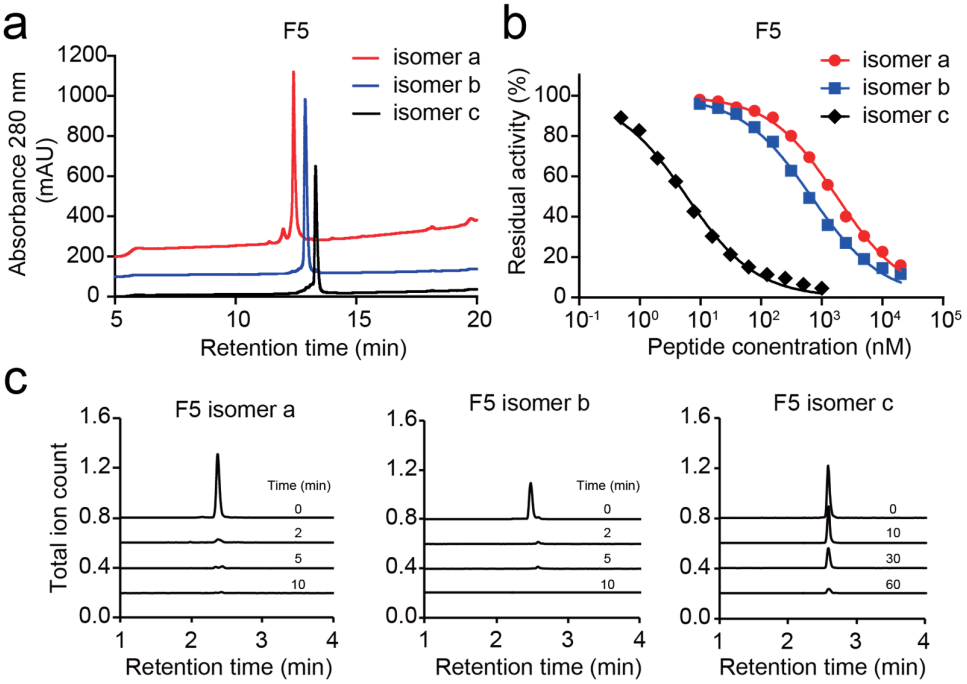

Supplementary Figure 6 Characterization of the three isomers formed upon cyclization of linear peptides, illustrated for peptide F5. a, Reversed-phase HPLC analysis of the three HPLC-purified isomers. The experiment was performed one time. **b,** Residual FXIa activity at different peptide concentrations. Means are based on two measurements. **c,** Remaining intact peptide after incubation in 100% SIF, analyzed by LC-MS. The total ion counts (TIC; in million) were recorded and are indicated. Experiments were repeated two times independently and similar results were obtained.

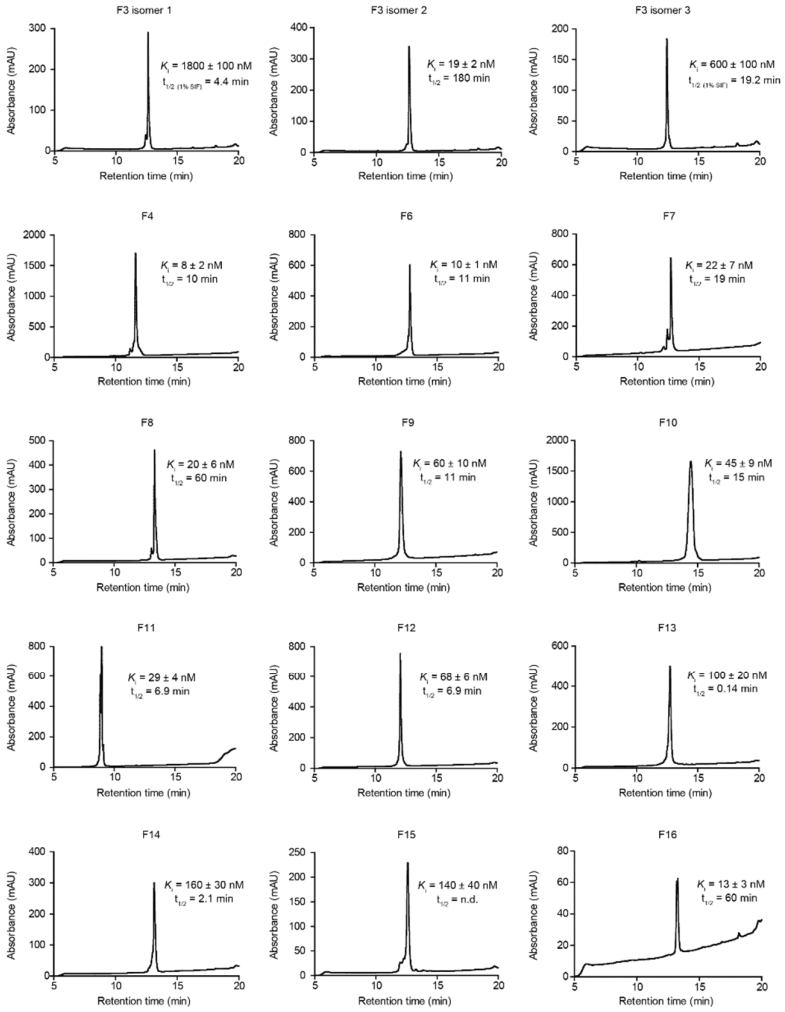

Supplementary Figure 7 Purity, activity and stability of double-bridged peptides. The peptides F3 isomer 1, 2, 3, F6 isomer 2, F19 isomer 2, F20 isomer 2, I1 isomer 1, 2, 3 and I5 isomer 3 were synthesized by step-wise removal of the protecting groups and cyclization with reagent **7**. All other peptides were obtained by reacting unprotected peptides with reagent **7** and HPLC-purification of the isomers. For peptides synthesized with this second strategy, only data for the most active isomer is shown. All peptides were analyzed by analytical HPLC. Mean values and SD of K_is for human FXIa and K_ds for IL-23R binding peptides were calculated based on three measurements. The stabilities in 100% SIF are indicated. Mean values were calculated based on two measurements.

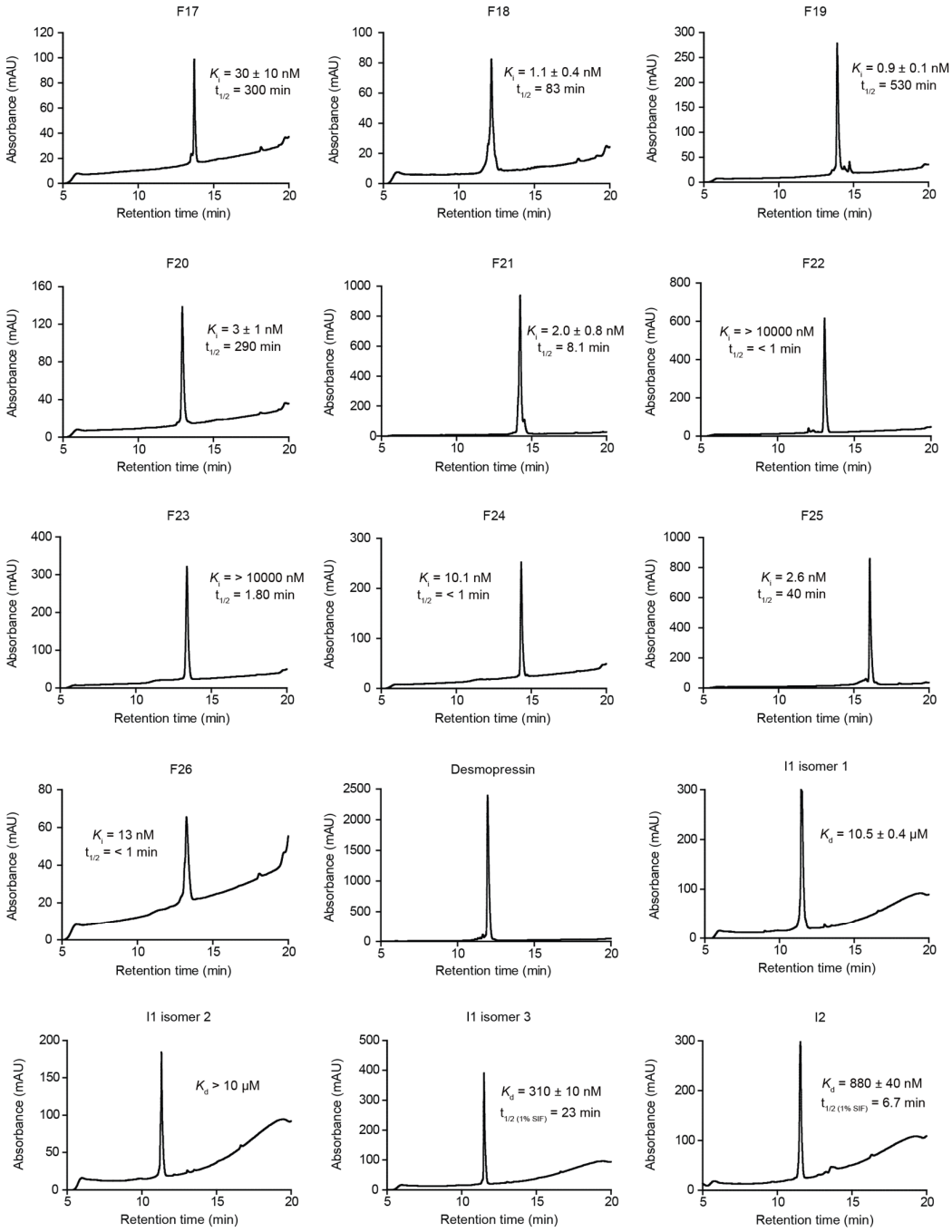

Supplementary Figure 7 Continued

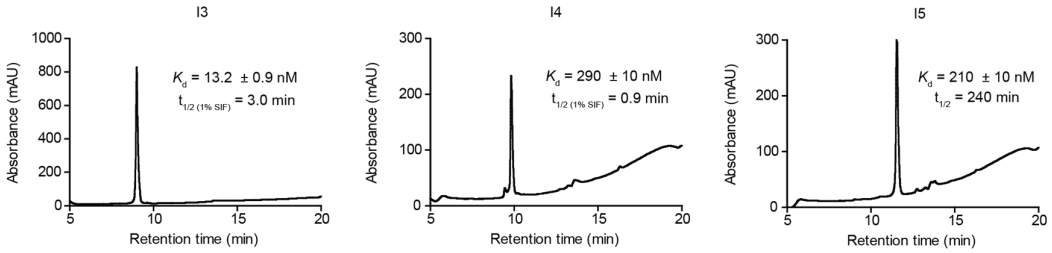

Supplementary Figure 7 Continued

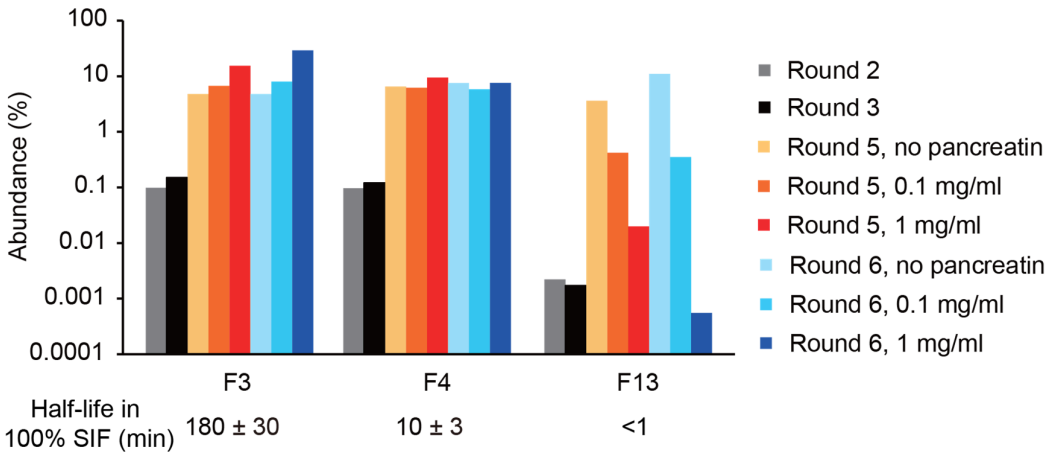

Supplementary Figure 8 Efficiency of protease stability selection. Abundance of three peptides with different stabilities in the different rounds of phage selection. Abundance was determined by sequencing 0.5 to 2 million clones per selection round and condition, and indicated as percentage of total sequences.

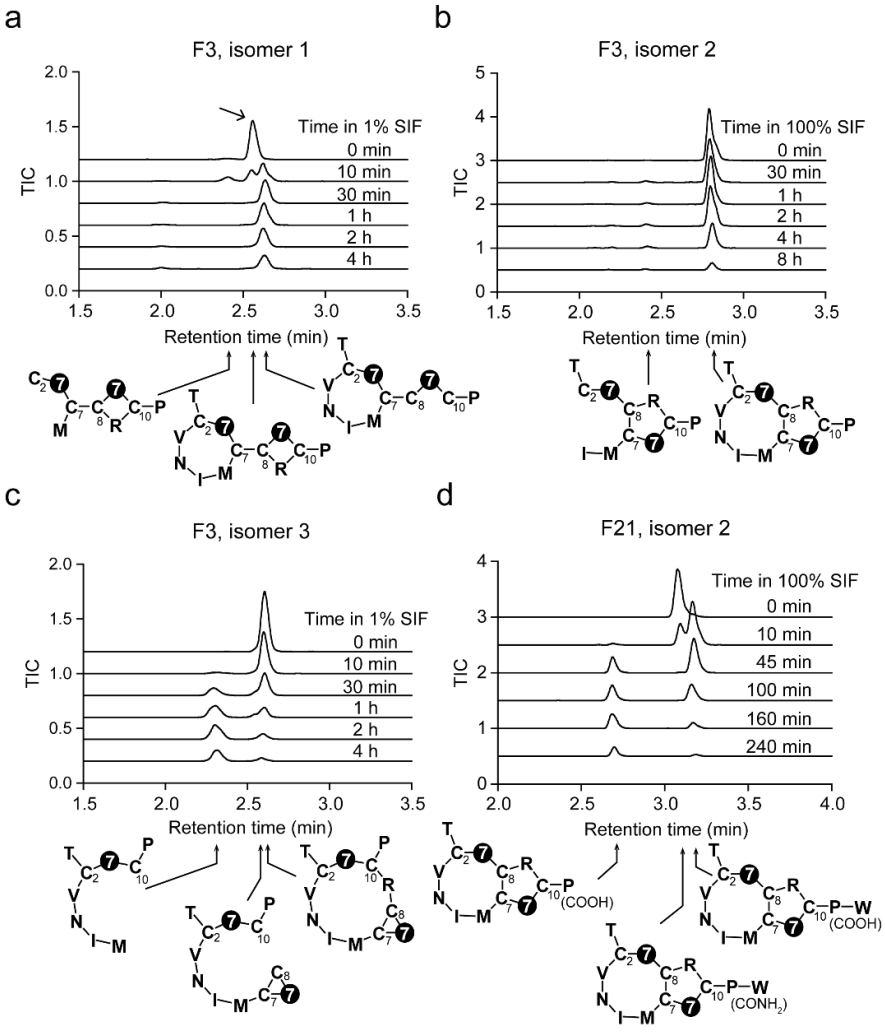

Supplementary Figure 9 Stability of peptides toward pancreatic proteases. The three isomers of the double-bridged peptide F3 (**a**-**c**) and isomer 2 of F21 (**d**) were incubated in 1% (isomer 1 and 3 of F3) or 100% SIF (isomers 2 of F3 and F21) at 37°C and analyzed by LC-MS. The total ion counts (TIC) were recorded and are indicated. Structures of the initial peptides and degradation products are shown. Experiments were repeated twice independently and similar results were obtained.

												K_i (nM)	$t_{1/2}$ (min)	aPTT
F3	T	C	V	N	I	M	C	C	R	C	P	19 ± 2	180	2.70
	E	C	V	N	I	M	C	C	R	C	P	26 ± 6	268	2.06
	T	C	E	N	I	M	C	C	R	C	P	16 ± 2	322	2.31
	T	C	P	N	I	M	C	C	R	C	P	50 ± 6	74	2.22
	T	C	V	S	I	M	C	C	R	C	P	40 ± 10	110	2.20
	T	C	V	N	I	F	C	C	R	C	P	3.9 ± 0.5	65	2.28
	T	C	V	N	I	4fF	C	C	R	C	P	24 ± 4	36	2.09
	T	C	V	N	I	hL	C	C	R	C	P	700 ± 100	n.d.	n.d.
	T	C	V	N	I	MO	C	C	R	C	P	> 1000	n.d.	n.d.
	T	C	V	N	I	MO_2	C	C	R	C	P	> 1000	n.d.	n.d.
	T	C	V	N	I	f	C	C	R	C	P	> 1000	n.d.	n.d.
	T	C	V	N	I	y	C	C	R	C	P	> 1000	n.d.	n.d.
	T	C	V	N	I	hF	C	C	R	C	P	> 1000	n.d.	n.d.
	T	C	V	N	I	PhG	C	C	R	C	P	> 1000	n.d.	n.d.
	T	C	V	N	I	M	C	C	nR	C	P	> 1000	n.d.	n.d.
	T	C	V	N	I	M	C	C	hR	C	P	> 1000	n.d.	n.d.
	T	C	V	N	I	M	C	C	4gF	C	P	> 1000	n.d.	n.d.
	T	C	V	N	I	M	C	C	R	C	βhP	29 ± 6	65	2.63
F18	T	C	V	N	I	M	C	C	R	C	p	1.1 ± 0.4	83	4.10
F21	T	C	V	N	I	M	C	C	R	C	P	W	2.0 ± 0.8	8.1	4.74

Supplementary Figure 10 Improving the affinity of peptide F3 by substituting amino acids with unnatural ones. Amino acid changes relative to F3 are indicated by black frames. K_i values for human FXIa, half-lives in 100% SIF at 37°C, and activated partial thromboplastin times (aPTT; prolongation at 30 μM peptide relative to control) are indicated. Mean values and SD for three measurements are shown for K_i values. Mean values for two measurements are shown for half-lives and aPTT. Abbreviations of unnatural amino acids: 4fF = 4-fluorophenylalanine, hL = homoleucine, MO = methionine sulfoxide, MO_2 =methionine sulfone, f = D-phenylalanine, y = D-tyrosine, hF = homophenylalanine, PhG = phenylglycine, nR = norarginine, hR = homoarginine, 4gF = 4-guanidinophenylalanine, βhP = β-homoproline.

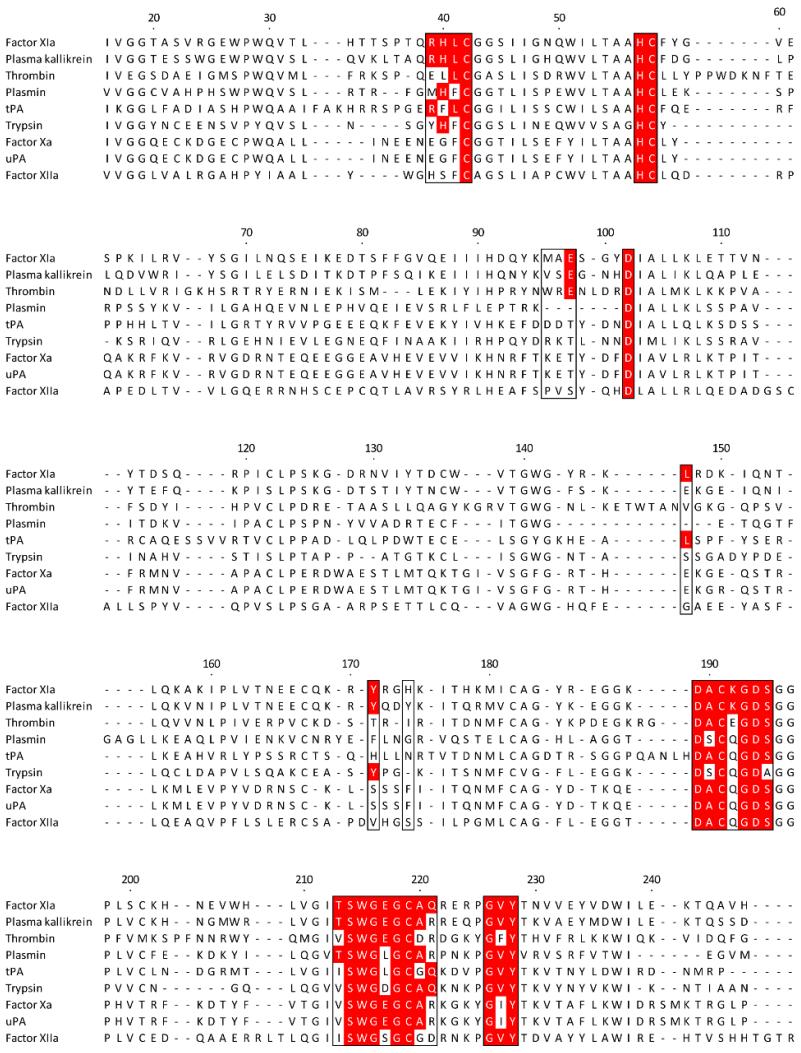

Supplementary Figure 11 Sequence alignment of FXIa catalytic domain with the catalytic domains of homogenous human proteases. The indicated amino acid numbers are based on the chymotrypsin numbering system. Amino acids of FXIa that are within 5 Å distance from the F19 inhibitor (based on PDB ID 6TWB) are marked by black frames. Amino acids in these regions that are identical in FXIa are highlighted in red. tPA = tissue-type plasminogen activator, uPA = urokinase-type plasminogen activator.

a

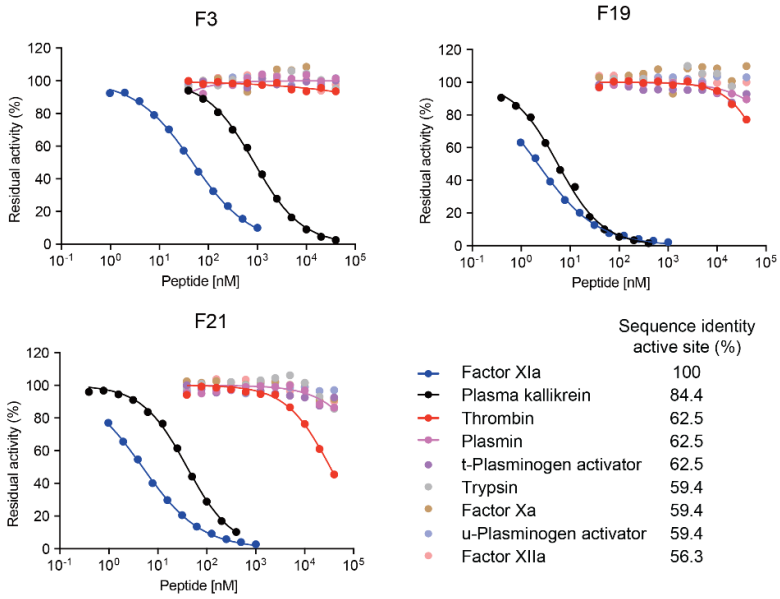

b

	K_i (nM)			
	F3	F19	F20	F21
Factor XIa	19	0.9	3.4	2.0
Plasma kallikrein	660	4.3	11.9	29
Thrombin	>40,000	>40,000	>40,000	26,000
Plasmin	>40,000	>40,000	>40,000	>40,000
t-Plasminogen activator	>40,000	>40,000	>40,000	>40,000
Trypsin	>40,000	>40,000	>40,000	>40,000
Factor Xa	>40,000	>40,000	>40,000	>40,000
u-Plasminogen activator	>40,000	>40,000	>40,000	>40,000
Factor XIIa	>40,000	>40,000	>40,000	>40,000

c

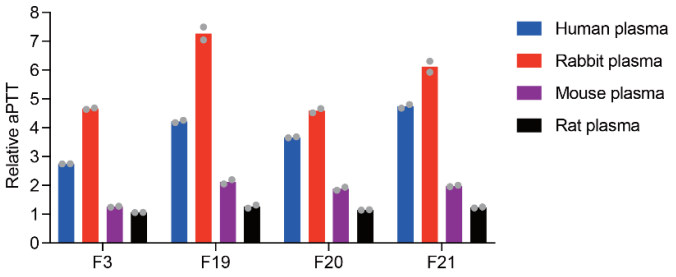

Supplementary Figure 12 Specificity of FXIa inhibitors. a, Inhibition of human FXIa and eight structurally related trypsin-like serine proteases by F3 and F3 derivatives. Average values of two measurements are indicated. The similarity of the proteases to FXIa is illustrated by indicating the percentage of amino acids around the active site

that are identical between FXIa and the tested proteases. For calculating the sequence identity, 32 amino acids in close proximity to the active site and on the protease's surface, indicated in Supplementary Fig. 11 with black frames, were compared. **b,** K_i values calculated based on the inhibition data shown in panel **a**. **c,** The inhibition of rabbit, mouse and rat FXIa was estimated by testing the inhibition of the intrinsic coagulation pathway in plasma of these animals. The aPTT, being the time to coagulation upon activation of the intrinsic coagulation pathway in blood plasma, was measured in presence of 30 μM F3, F19, F20 or F21. The ratio of the measured aPTT with and without inhibitor is indicated. Average values of two measurements are shown. The dots in gray indicate the values of the two measurements.

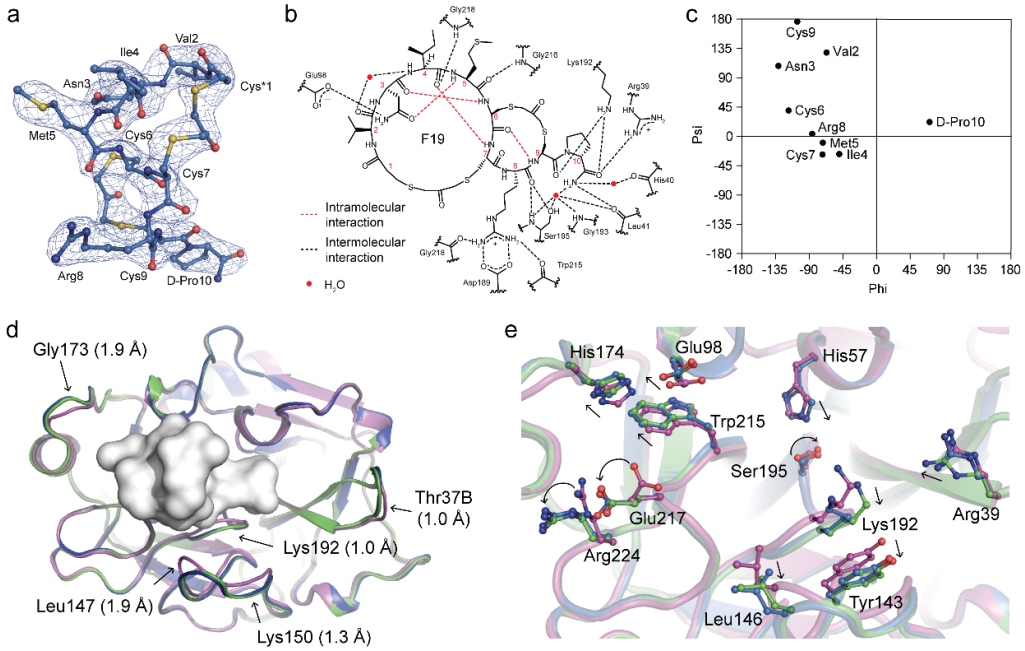

Supplementary Figure 13 X-ray structure of F19 bound to FXIa catalytic domain (PDBID: 6TWB). a, 2fo-fc electron density map of F19 contoured at a 1.5σ level. **b,** Intra- and intermolecular hydrogen bonds formed by F19. **c,** Ramachandran plot of F19. The backbone dihedral angles in the crystal structure 6TWB were measured in Pymol. Amino acids 4 to 8 locate in the region of a right-handed helix. **d-e,** Comparison of the catalytic domain of FXIa bound to F19 (PDBID: 6TWB, green), F21 (PDBID: 6TWC, blue) and benzamidine (PDBID: 1ZHM, rose). Amino acids that have different backbone **d** or side chain conformations **e** upon binding of a double-bridged peptide versus benzamidine are indicated. F19 is shown with a white surface in **d**. Distance of backbone movement between 6TWB and 1ZHM are shown in brackets.

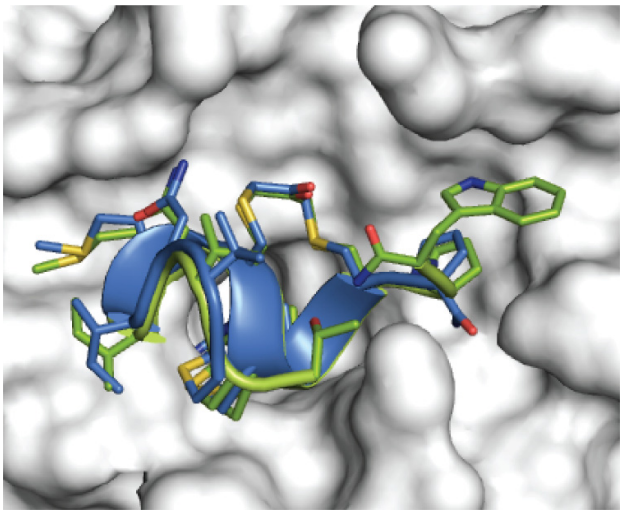

Supplementary Figure 14 Comparison of F19 and F21 bound to FXIa. The X-ray structure of F21 (green, PDBID: 6TWC) bound to FXIa is shown and the structure of F19 (blue, PDBID: 6TWB) is overplayed for comparison.

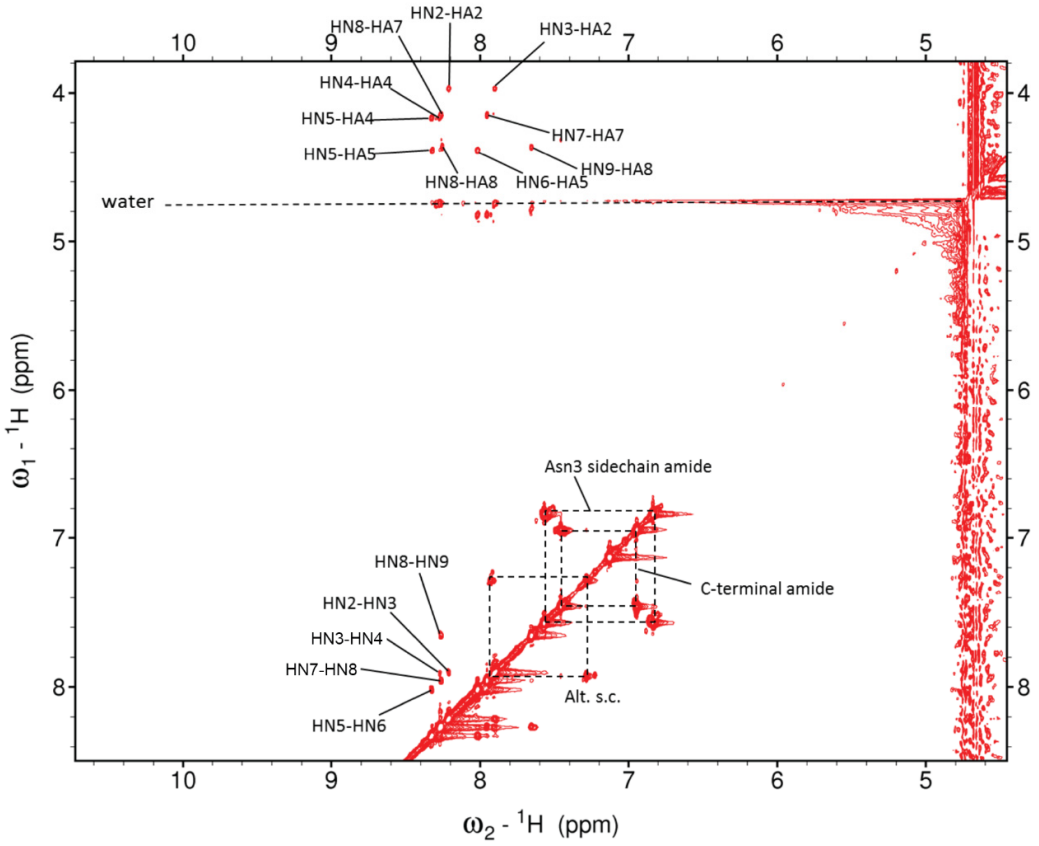

Supplementary Figure 15 ^{1}H-^{1}H NOESY spectrum of F19. The region shown spans HN-HN and HN-HA correlations, where crosspeaks between HA and HN resonances of i – i+3 and i – i+4 residues are expected for helical conformations. For correlations between backbone nuclei, crosspeak labels are formatted ω2 (x axis, direct ^{1}H dimension) – ω1 (y axis, indirect ^{1}H dimension) using either HN for amide ^{1}H or HA for alpha ^{1}H, followed by the residue number. Dashed boxes indicate N-H_2 correlations from sidechains and the C-terminus. Alt. s.c. refers to a strong geminal coupling from either Asn3's sidechain or the C-terminal amide in a minor species. The experiment was performed once.

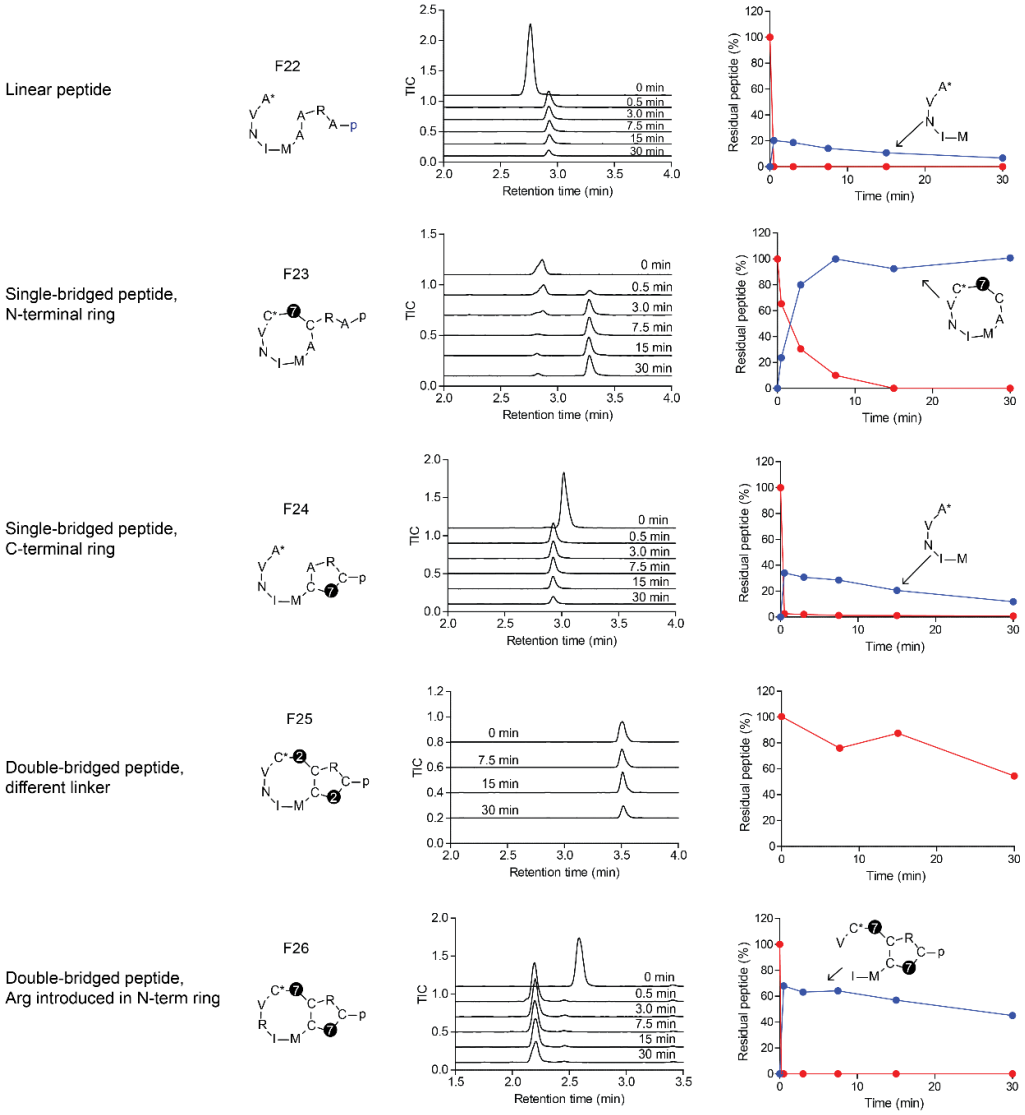

Supplementary Figure 16 Stability of linear, monocyclic and bicyclic derivatives of F19. The indicated peptide formats were incubated for 30 min in 100% SIF and samples at different time points analyzed by LC-MS. The total ion count (TIC) was recorded and is shown. The % peptide remaining intact at the different time points is shown in red (average values of two measurements). The major degradation products observed are shown in blue (average values of two measurements). Experiments were repeated two times independently with similar results.

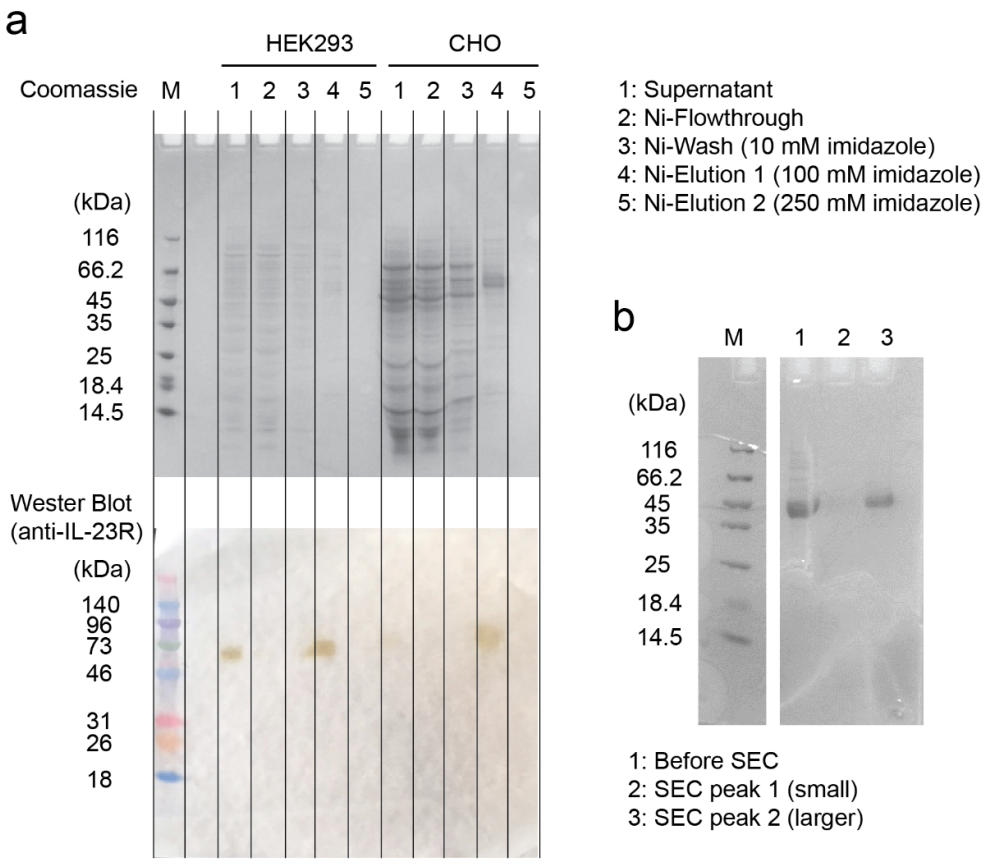

Supplementary Figure 17 Expression and purification of IL-23R. a, Comparison of expression in HEK293 and CHO cells, and purification by Ni-NTA affinity chromatography. **b,** Second purification of IL-23R by size exclusion chromatography (SEC). The expression and purification were done two times independently with similar results.

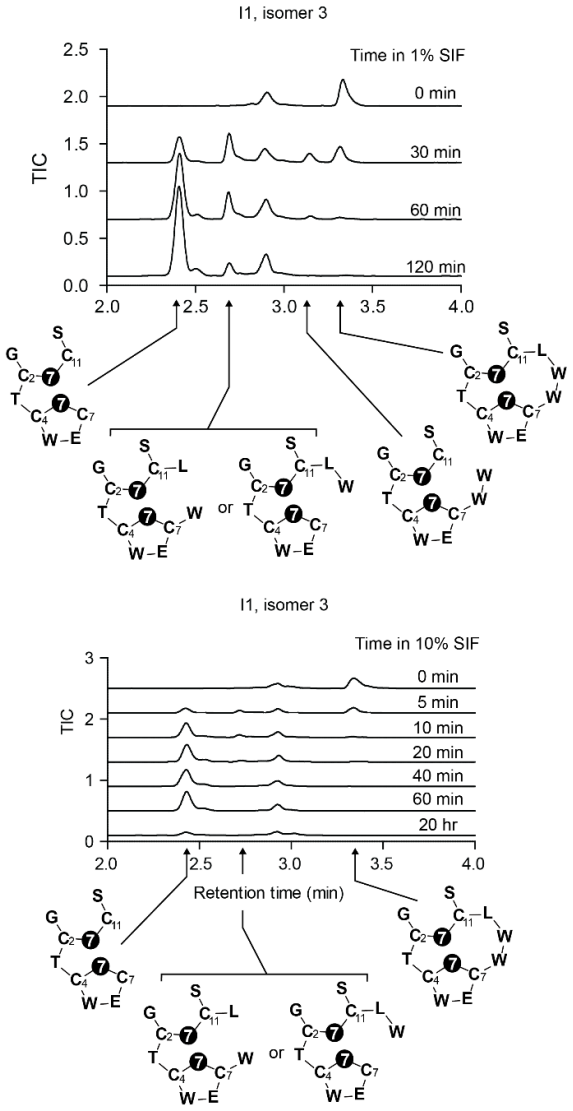

Supplementary Figure 18 Degradation pathway of peptide I1. The peptide I1 (isomer 3) was incubated in 1% or 10% SIF at 37°C and analyzed by LC-MS. The total ion counts (TIC) were recorded and are indicated. Structures of the initial peptides and degradation products are shown. Experiments were repeated two times independently with similar results.

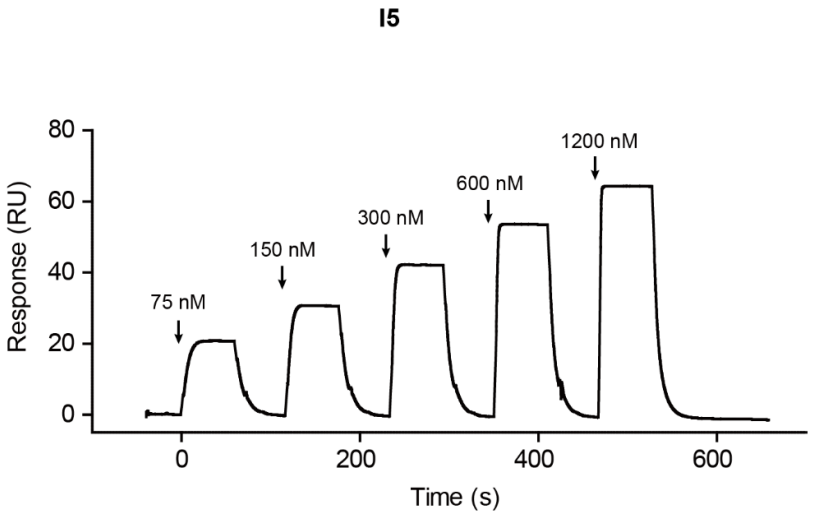

Supplementary Figure 19 Binding affinity of peptide I5 measured by SPR. One out of three recorded single cycle SPR sonograms of peptide I5. IL-23R was immobilized and I5 was injected at the indicated concentrations. Experiments were repeated three times independently with similar results.